processes

Article

Analysis and Optimization of the Fuel Consumption of an Internal Combustion Vehicle by Minimizing the Parasitic Power in the Cooling System

Pedro H. A. Brayner [1], José Â. P. da Costa [1,2], Alvaro A. V. Ochoa [1,2,*], José J. Urbano [2], Gustavo N. P. Leite [1,2] and Paula S. A. Michima [1]

[1] Department of Mechanical Engineering, Federal University of Pernambuco, Cidade Universitaria, 1235, Recife 50670-901, Brazil; pedrobrayner@gmail.com (P.H.A.B.); angelocosta@recife.ifpe.edu.br (J.Â.P.d.C.); gustavonovaes@recife.ifpe.edu.br (G.N.P.L.); paula.michima@ufpe.br (P.S.A.M.)

[2] Department of Higher Education Courses (DACS), Federal Institute of Education, Science and Technology of Pernambuco, Av. Prof Luiz Freire, 500, Recife 50740-545, Brazil; josejunio@recife.ifpe.edu.br

* Correspondence: ochoaalvaro@recife.ifpe.edu.br; Tel.: +55-81-99976-4266

Abstract: This study aims to enhance energy efficiency by reducing parasitic losses in the engine cooling system through a new drive strategy involving a two-stage water pump and a variable electro-fan. The fuel consumption gain analysis focused on a vehicle with average characteristics typical of 1.0L hatchbacks in the Brazilian market and urban driving conditions. The methodology implemented aims to minimize power absorbed by the forced water circulation and thermal rejection, thereby reducing parasitic losses, particularly during low-speed urban driving, without causing air-side heat exchanger saturation. The results show a potential decrease of up to 80% in power absorbed by the cooling system, leading to an estimated fuel consumption saving of approximately 1.4% during urban driving cycles.

Keywords: energy efficiency; fuel consumption; parasitic power; cooling system

Citation: Brayner, P.H.A.; da Costa, J.Â.P.; Ochoa, A.A.V.; Urbano, J.J.; Leite, G.N.P.; Michima, P.S.A. Analysis and Optimization of the Fuel Consumption of an Internal Combustion Vehicle by Minimizing the Parasitic Power in the Cooling System. *Processes* **2024**, *12*, 321. https://doi.org/10.3390/pr12020321

Academic Editor: Cherng-Yuan Lin

Received: 21 December 2023
Revised: 29 January 2024
Accepted: 31 January 2024
Published: 2 February 2024

1. Introduction

The historical development of combustion engines has been marked by increased power density, torque, and working rotation speeds, which have led to higher thermal rejection. To maintain efficient and safe operation, the propulsion components within the system must reach their ideal working temperatures quickly [1]. In this way, the aim is to avoid high temperatures, which can cause detonation problems or require engine protection strategies, and low temperatures, which result in higher lubricant viscosity and increased losses due to internal friction [2]. Hence, the vehicle's cooling system must consider its role in critical situations where additional heat could cause localized heating in specific components, resulting in material damage [3]. This issue mainly occurs under full engine load conditions and can be mitigated by circulating coolant at high speeds. However, outside these conditions, the system tends to be oversized, leading to high hydraulic losses when under partial load. As a result, cooling systems have undergone numerous improvements to increase cooling capacity to compensate for the engine's thermal rejection [2–4]. However, this increase is associated with high energy consumption [3].

Several measures have been implemented to mitigate the rise in energy consumption, particularly fuel usage and CO_2 emissions. This increase can generally be addressed by considering two alternatives. The first involves labeling programs designed to enhance competitiveness by providing consumers with comparative information on the fuel consumption of new vehicles in the market. The second alternative is through energy efficiency programs, which impose minimum consumption improvement requirements on automakers' fleets. These programs usually impose penalties if the specified targets are not achieved and sometimes offer incentives to companies that surpass certain targets [5,6].

There is significant interest in the automotive industry in optimizing energy consumption related to cooling, focusing on minimizing the parasitic power consumed in this process [7,8]. Furthermore, several production applications already incorporate solutions such as PWM electro-fans, brazed radiators with complex geometry and high efficiency, controlled thermostatic valves, and variable water pumps [9,10]. However, implementing new technologies and more complex solutions in the automotive industry can be costly [11,12].

Although the implementation of stricter emissions regulations has encouraged the search for various energy efficiency technologies, two major groups of technologies are being studied and implemented. The first is focused on reducing the vehicle's energy demand, which can be achieved through vehicle demand energy (VDE) strategies. The second group is related to the propulsion system's efficiency, which can be improved through propulsion system efficiency (PSE) technologies [13].

Cipollone et al. [14] conducted a comparative analysis by replacing traditional centrifugal pumps in automotive cooling systems with a vane-type water pump. The research was based on the influence of the speed of centrifugal pumps on efficiency, with maximum values of 45% to 50% near the engine's full power region (high speeds) and a decrease in efficiency to levels of 15% to 20% at lower speeds, corresponding to the consumption homologation cycles. Similarly, Fatigati et al. [15] analyzed an IVECO 3.0 L turbodiesel engine to optimize the geometry and ideal positioning of the vane pump through the inlet and outlet. The study revealed that a design with a disk aspect demonstrated superior performance, primarily due to reduced internal friction. This led to a decrease in specific CO_2 emissions of 0.4 g/km when the flow rate was regulated by the eccentricity of the pump with a direct mechanical drive of the engine and 1.4 g/km when the speed of the pump regulated the flow rate through the electrical drive of the pump. Naderi et al. [16] proposed an intelligent control system for a pump with an electric drive based on the load-rotation map obtained from a thermal simulation model of the engine and cooling system. The most significant results of the study were a 44% reduction in the pump's drive power and a 2.0% reduction in fuel consumption. In a survey by Haghighat et al. [17], an intelligent thermal management control model was developed for a 1.4 L gasoline (70 kW/125 Nm) and natural gas (62 kW/111 Nm) engine. This model used an electric pump, a heated thermostatic valve, and a two-speed electro-fan. The control system aimed to find the most efficient operating condition depending on the engine load. Turabimana et al. [18] developed a computer model of an active cooling system for an internal combustion engine using a thermostatic valve to quickly change the direction of the coolant flow and maintain the coolant temperature within the appropriate range. The proposed engine cooling system had several advantages, including stable pressure in the upper radiator hose, the engine operating at a consistent temperature, the electric current required being less than 1A to activate the thermostat valve, and the engine components not wearing out due to the engine overheating. In the same context, and using a 1.5 L naturally aspirated vehicle, Yuan et al. [19] developed a simplified computer model on the Amesim platform. The performance of the engine's cooling system was simulated using extremely cold and normal temperature conditions. The simulation results showed that the radiator row number significantly impacts the cooling system performance; the water pump transmission ratio and the radiator area also play an important role. Also applying a computational analysis, Addo et al. [20] investigated the impact of removing the coolant thermostat on a car engine's performance. Predictive models were created using machine-learning techniques to assess the engine's performance with and without a coolant thermostat. Removing the thermostat led to a 32% decrease in the engine's coolant temperature and a 29% decrease in the automatic transmission's oil temperature. The total fuel consumption increased by 40%, and the car engine's carbon monoxide emissions rose by 737%.

Faraj et al. [21] found that using diffusers between the front of a car and the heat exchanger subjected to airflow reduced fuel consumption and the vehicle's pollutant emissions. The study showed that the intensity of the air velocity was reduced but distributed over a larger surface area of the exchanger, leading to greater thermal performance. For a car with engine power ranging from 100 to 200 kW, used three hours a day, and equipped with a diffuser, there is a reduction of up to 2.90 kg (3.90 L) of gasoline consumption and 9.51 kg of CO_2 emissions per day.

Another alternative to reduce fuel consumption is thermal management methods, as shown by Salehi et al. [22], such as a thermal management approach and a map-controlled thermostat. A map-controlled thermostat has been shown to reduce a vehicle's average fuel consumption by around 2.0% compared to current cars with standard thermostats. Gupta et al. [22] analyzed the benefit of maintaining a higher coolant temperature at medium loads, its influence on fuel economy, and its relationship with friction reduction and cooling losses. Kalinichenko et al. [23] proposed an analysis of various waste heat recovery technologies for the vehicular agricultural sector using technical and economic indicators. It was found that turbocharging, electric turbocharging, and transmission oil heating configurations for hydraulic clutch gearboxes were effective for agricultural vehicles with a different operating cycle than road trucks.

A study on the potential of enhancing vehicle cooling systems using nanofluids was conducted in the literature [24–26]. The analysis focused on the behavior of these nanoparticles to increase efficiency. Using nanofluids presented the opportunity to reduce the size and weight of the radiator. The potential of introducing a phase change material (PCM) to equalize thermodynamic processes was explored. The introduction of PCM resulted in a better temperature balance, leading to improved engine efficiency [24].

Like engines, cooling systems have undergone numerous enhancements to enhance their cooling efficiency to offset the rise in engine thermal rejection. Nevertheless, this escalation is typically linked to a heightened level of energy consumption. In this context, there is significant interest within the automotive sector in optimizing energy consumption associated with the cooling system, as reflected in the literature [7–9]. The primary focus has consistently been on minimizing the parasitic power consumed during this process. This research responds to the crucial demand for economical solutions within the automotive sector, where opportunities for optimization and precise control are often limited. It further offers a novel methodology for diminishing fuel consumption in small vehicles by applying scientific techniques.

The research introduces an innovative approach to enhance energy efficiency by addressing parasitic losses in the engine cooling system. The manuscript's novelty lies in its proposition to optimize energy consumption in a compact vehicle by introducing a new control system for the water pump and a pulse width modulation (PWM) electric fan. The main contributions are:

- ✓ Formulate an analytical calculation model to quantify the fuel consumption reduction attributed to the diminished parasitic power of the cooling system.
- ✓ Investigate fuel consumption improvements in a compact vehicle featuring a 1.0 L cylinder capacity, particularly under urban traffic conditions.
- ✓ Conduct simulations to assess the reduction in parasitic losses and improvements in fuel consumption under various driving cycles, incorporating the newly proposed control strategy.
- ✓ Perform a comparative analysis by juxtaposing the outcomes of this study with findings from relevant works in the State of the Art, emphasizing key distinctions and contributions.

2. Energy Analysis of Internal Combustion Vehicle Performance

This section will show the vehicle test procedure to determine fuel consumption, the types of driving cycles adopted in the analysis, the reference base vehicle, and the implementation steps of the adopted methodology [26].

2.1. Test Procedure and Determination of Fuel Consumption

The official consumption values of a vehicle are obtained through measurements on a chassis dynamometer through the PBEV (Brazilian Vehicle Labeling Program). The chassis dynamometer simulates the resistive forces of the car on the track by NBR-10312 [27] and, through the collection and analysis of exhaust gases emitted by the engine, allows the determination of fuel consumption during the test through carbon balance calculations.

Tests in Brazil strictly follow the procedures contained in standard NBR 6601 [28] being carried out under controlled conditions of ambient temperature between 20 and 30 °C, requiring a minimum period of 12 h for vehicle acclimatization and a maximum time between vehicle testing—thirty-six hours—so that the vehicle is pre-conditioned and at room temperature at the start of the tests.

To carry out the test, a driver drives the vehicle on the dynamometer smoothly and with minimal movement of the accelerator pedal, and gear changes are carried out as the test requester recommends in cars with manual transmission. A driver is responsible for driving the vehicle according to specific speed profiles, known as driving cycles, constituting a standard simulation of urban and/or highway use conditions on public roads following NBR 6601 [28]. The exhaust pipes are mounted to a CVS (constant volume sampler) that collects and dilutes exhaust gases in sampling bags that are conditioned and subsequently analyzed.

The emissions analyzer equipment is a set of analytic systems such as a flame ionization detector (FID), non-dispersive infra-red (NDIR), chemiluminescence detector (CLD), and selective catalytic reduction (SCR). The analyzer calibration and operation follow the NBR 6601 [28] to determine the concentration of the pollutants. During the test, exhaust gases from the vehicle's exhaust are collected in sampling balloons (watertight bags) and subsequently analyzed to obtain pollutant emission levels following NBR 6601 and fuel consumption by NBR 7024 [29]. The consumption value (in L/100 km) is determined through the masses of HC, CO, CO_2, and unburned ethanol based on the carbon balance calculation according to Equation (1).

$$C = \frac{(0.8656 \cdot m_{HC}) + (0.5214 \cdot m_{ETOH}) + (0.4288 \cdot m_{CO}) + (0.2729 \cdot m_{CO2}) \cdot (100 + \%V_{H2O})}{(6.4487 \cdot \%V_{gs}) + (4.1105 \cdot \%V_{ETOH})} \quad (1)$$

The following values were used to calculate the average energy consumption value in MJ/km: density values of Gasool A22, which is the mixture of 78% by volume of pure gasoline with 22% by volume of anhydrous Ethanol, also known as E22. This is the standard fuel adopted for gasoline consumption tests in Brazil, as specified in the standard [29]. Table 1 shows the characteristic of reference fuels specified in Brazil.

Table 1. Characteristics of reference fuels specified by ANP [29].

		E00	E22	E100		VNG
Calorific Power	MJ/kg	43.06	38.92	24.80	MJ/kg	48.74
Density	kg/L	0.735	0.745	0.810	kg/Nm^3	0.723
Energy Density	MJ/L	31.65	28.99	20.09	MJ/Nm^3	35.24

However, fuel consumption in Brazil is determined by the value of fuel range (in km/L). These values, officially published in the PBEV—Brazilian Vehicle Labeling Program, are calculated according to consumption according to Equation (2).

$$A = \frac{100}{C} \quad (2)$$

2.2. Driving Cycles

Among the best-known driving profiles are the cycles of the North American Environmental Protection Agency—EPA [30], which uses the FTP75—Federal Test Procedure cycle as an urban traffic configuration, and the cycle Highway Fuel Economy Driving Schedule—HWFET [30,31] representing extra-urban or road conditions. These cycles are used as standard not only in the United States but also in Brazil and some other countries.

Alternatively, several countries use the New European Driving Cycle—NEDC [32]. This is a mixed cycle, composed of urban phase 1, which consists of four repetitions of the Urban Driving Cycle—UDC [33] plus one repeat of the Extra-Urban Driving Cycle—Emission Test Cycles: Worldwide engine and vehicle test cycles; phase 2 of extra-urban driving [33] difficulty with consumption and emissions tests in the laboratory is the significance of the cycle profile compared with the traffic reality that the driver encounters daily. The Worldwide Harmonized Light Vehicles Test Procedure—WLTP cycle was developed as shown in the literature [34], which does not present a classic configuration with urban and road phases only but has four distinct stages that seek to cover a broader range of conditions in which the customer uses the vehicle. This cycle aims to replace the NEDC cycle in the vehicle emissions and consumption approval processes in the European Union.

Similarly, the RTS95 cycle has three urban, rural, and highway regions. This cycle has an aggressive profile and has been used as a reference for development focused on the real driving emissions (RDE) condition. It is considered a good representation of the limiting conditions of a dynamic driving profile, approaching the "worst case" for the driving system—engine emissions control. Other driving profiles seek, for example, to replicate, more specifically, the typical traffic conditions of a given city, as is the case with the LA92 and NYCC cycles. The first portrays conditions in Los Angeles, California, and the second reproduces the intense traffic conditions in New York City.

Finally, the Artemis Cycle urban profile is also used, developed based on numerous databases of real European driving patterns. All results presented in this work will be evaluated for each cycle to give a spectrum of consumption benefits under different driving conditions.

2.3. Reference System—Base Vehicle

The proposal of this work will be compared with a base vehicle that only has a typical centrifugal water pump, with rotation proportional to the engine rotation, without any controllable flow variation mechanism [26]. The vehicle used in this study is a flex fuel, and Brazilian legislation requires testing with two fuels, E22 and E100; however, the analysis was carried out with E22 fuel. Table 2 below presents the characteristics of the base vehicle compared to the proposed vehicle.

Table 2. Qualitative characteristics of the base vehicle versus the proposed vehicle.

Actuator	Characteristics	BASE Vehicle	PROPOSED Vehicle
Water pump	Type of mechanism	Mechanical	Mechanical
	Speed control	Fixed ratio (X:1)	Variable of two reasons (X:1/2X:1)
Fan	Type of mechanism	Electric	Electric
	Speed control	PWM	PWM

First, a model for calculating thermal rejection and parasitic power in the cooling system was developed, obtaining the results from the base and proposed vehicles for the same fixed operating points. Based on these results, a comparative assessment of the efficiency of the two systems was carried out by mapping each operating point, making it possible to define a proposed control strategy for the cooling system that optimizes energy efficiency. Finally, a complete calculation model was generated that allows the calculation of the fuel consumption delta for a given driving cycle when the proposed strategy is applied. Figure 1 shows the flowchart of the steps in the general process of the implemented methodology. The name basic refers to an auto segment in Brazil, the simplest ones one can usually get from an automaker.

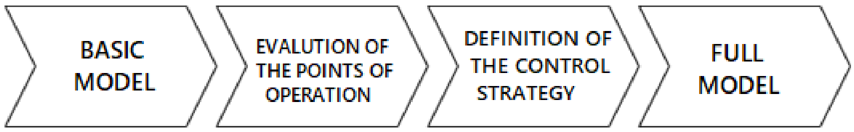

Figure 1. Steps of the implemented methodology.

3. Development and Implementation of the Methodology

The development and implementation of the methodology for optimizing fuel consumption in internal combustion vehicles were carried out through several stages, such as the development of the basic model, considering input variables and output results, set of intermediate data, and evaluation of operating points, followed by the development of the energy consumption model.

3.1. Basic Model

An analytical calculation model was created in Figure 2 to determine the value of thermal rejection in the radiator to the environment and the mechanical power absorbed by the cooling system. Based on this model, the base system's parasitic loss level can be compared with the proposed system for any imposed operating point, indicating the operating regions with the potential for improving efficiency without loss of thermal performance.

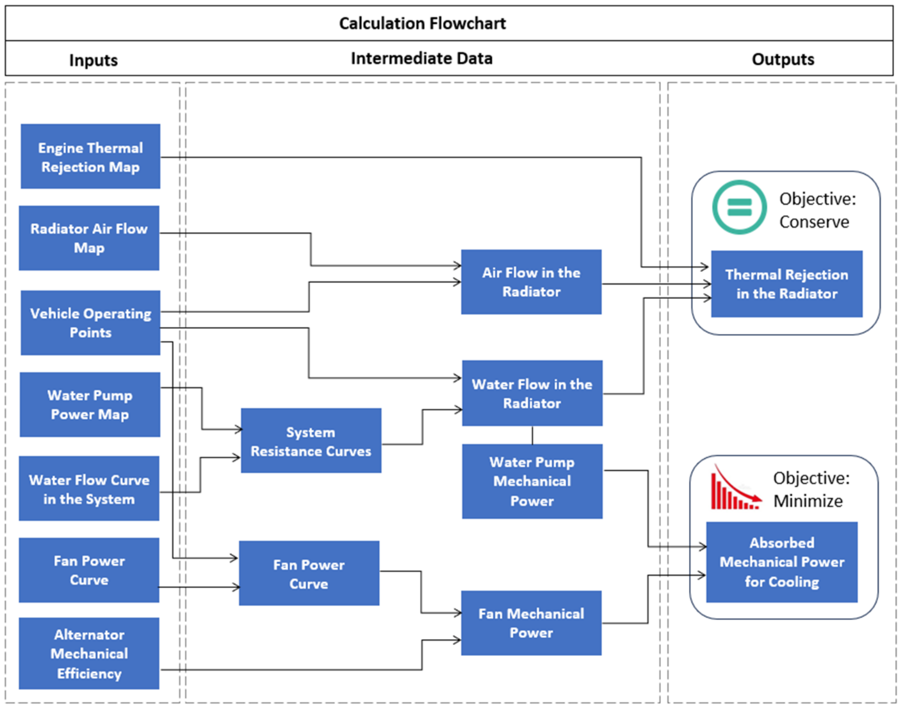

Figure 2. The flowchart is used to implement the basic energy calculation model.

3.2. Model Inputs

The primary information on the configuration of the vehicle under study was obtained directly from datasheets, manuals, physical measurements, virtual simulations, or engineering considerations. On average, the car in this segment weighs 1007 kg in running order. Regarding the engine, the usual application is a block with three cylinders in line and a head with 12 valves, equipped with a natural aspiration system, delivering maximum power in the order of 77 (gasoline) to 81 hp (ethanol) and peak torque in the range of 97 to 102 Nm (gasoline and ethanol, respectively).

Radiator thermal rejection map: The heat exchange map of the radiator shows the thermal power dissipated as a function of the speed of air and water flows through the heat exchanger. This is fundamental information for this analysis, as the vehicle's operating points on this map will indicate the effectiveness of increasing the flow of water or air in the radiator, Figure 3. As it is sensitive information, the radiator's heat exchange map was obtained through the component datasheet from the supplier.

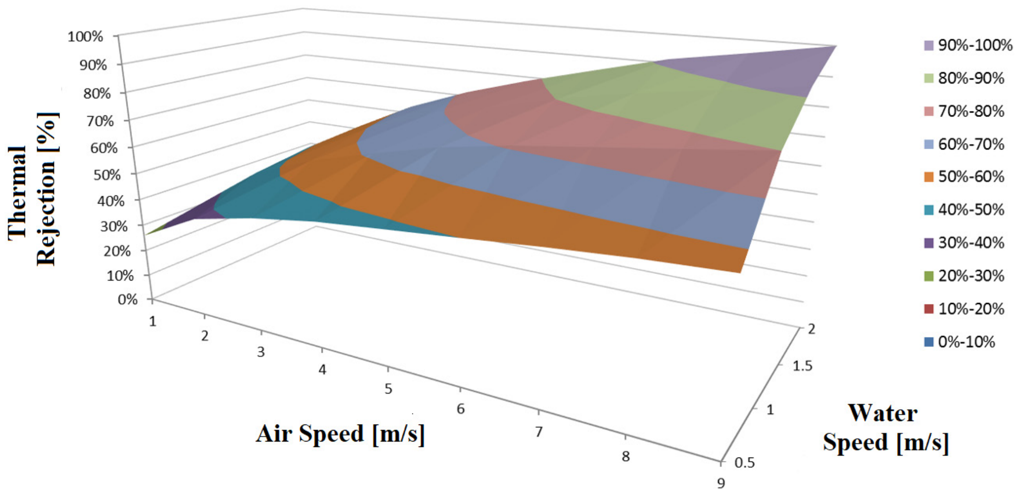

Figure 3. Heat rejection map of the radiator as a function of air and water flow.

Radiator thermal rejection map: Data were used from a 3D CFD computer simulation of the airflow in the engine compartment from a model from a car manufacturer in Brazil, including the entire front part of the vehicle, heat exchangers, and other elements present in the engine compartment. The results are shown as a map of average air speed through each heat exchanger in the vehicle's front package as a function of the vehicle's speed and fan rotation, Figure 4. As it is sensitive information, the radiator's heat exchange map was obtained through the component datasheet from the supplier. Dark shades correspond to lower values of fan speed, vehicle speed, and airflow through the radiator. On the other hand, lighter shades indicate higher values for these speeds.

Vehicle operating points: For the basic model, the operating points were imposed and represent all possible combinations of gear, vehicle speed in intervals of 1 km/h, and fan rotation at 250 rpm, as shown in Table 3. Each operating point also has its respective engine and water pump rotations. Brazilian Standard procedures were used to ensure the test conditions [27–29,35].

Table 3. Ranges mapped in the study.

March	Speed	Fan Speed
1st	10 to 40 km/h	0 to 2500 rpm
2nd	15 to 70 km/h	0 to 2500 rpm
3rd	25 to 100 km/h	0 to 2500 rpm
4th	35 to 160 km/h	0 to 2500 rpm
5th	40 to 160 km/h	0 to 2500 rpm

Water pump power map: The curves of power absorbed by the water pump as a function of its rotation and the system's total water flow were simplified by linear regressions, considering the measurements carried out by the manufacturer, Figure 5.

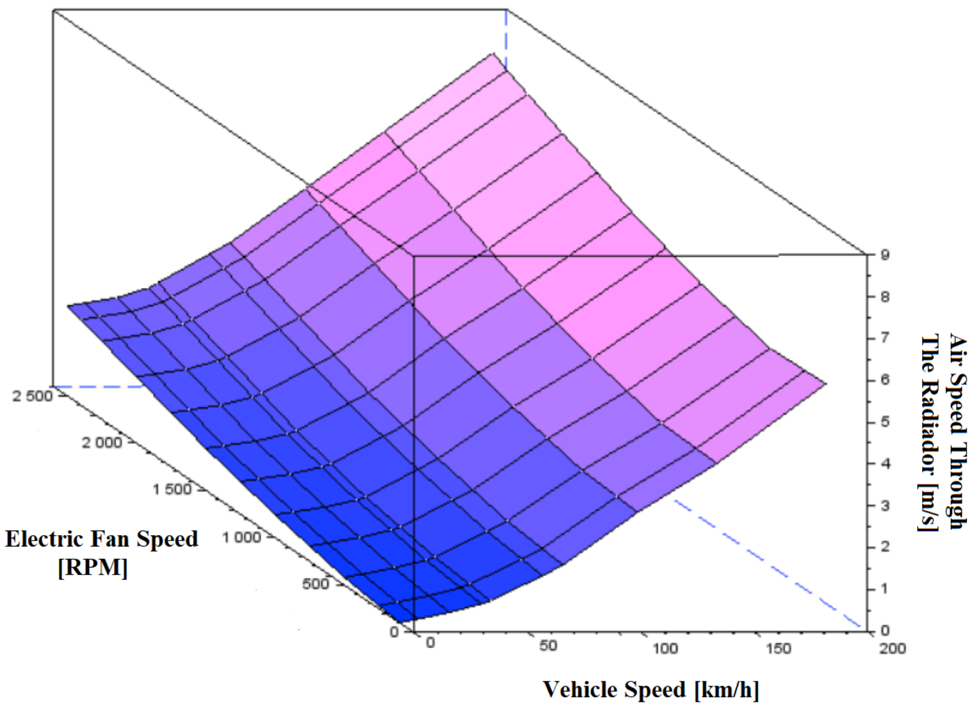

Figure 4. Map of average air speed through the radiator.

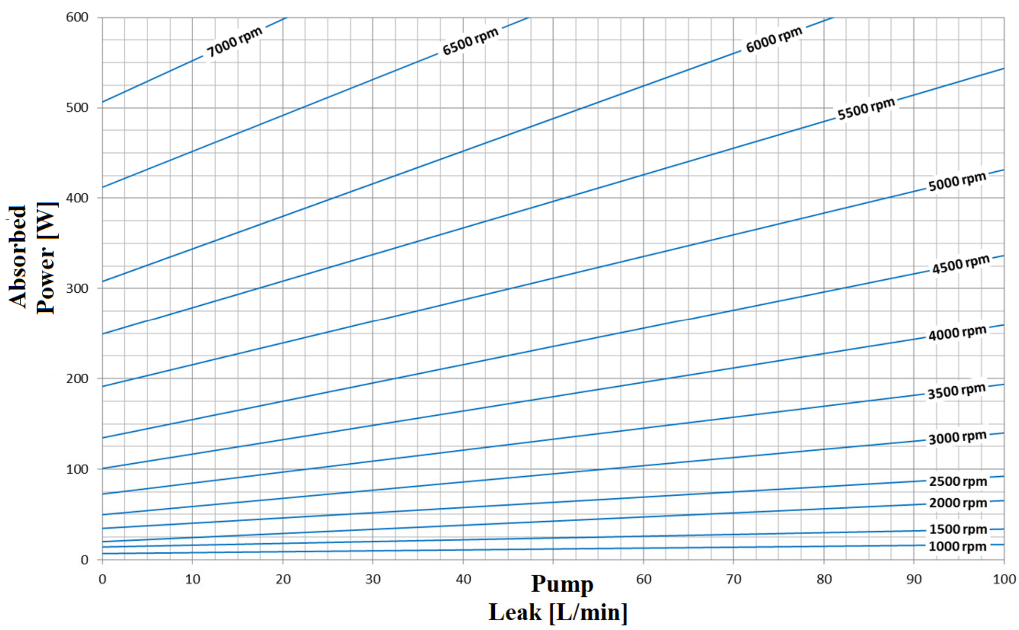

Figure 5. The water pump absorbs mechanical power curves.

Water flow curves in the system: The operating points of the water system were identified through flow measurement tests in the vehicle's cooling system, which uses a radiator, water pump, and an electric fan. Two measurements were carried out, one with the thermostatic valve completely closed and the other with the valve locked at its maximum opening. For the tests, the instrumentation shown in Figure 6 was utilized, which, among other items, has two turbine-type flow meters, one on the water pump and the other on the radiator, to obtain water flow values in the system. The tests ranged pump rotations from 1000 to 7000 rpm, totaling 11 measurement points (rotations) stabilized with 1 min duration each and three repetitions for each point.

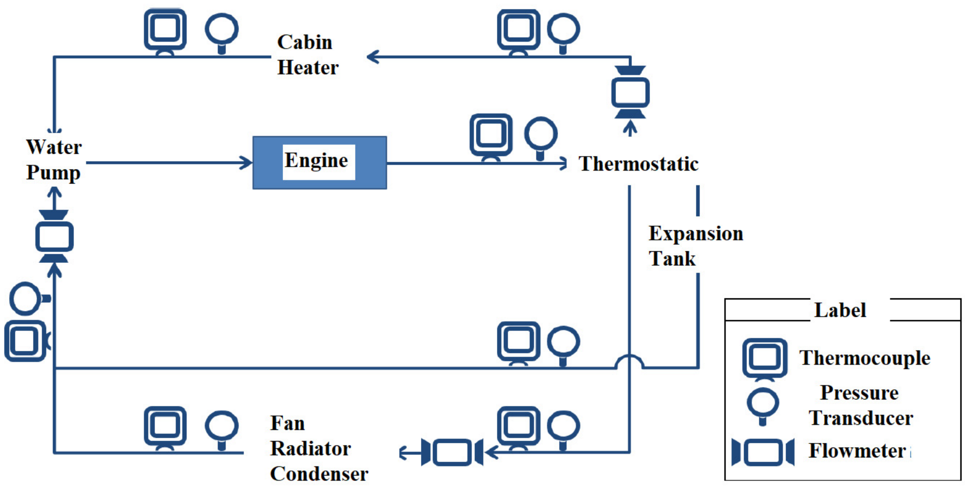

Figure 6. Test instrumentation schematic.

Fan power curve: The electric fan used as a reference for this work has a nominal power of 300 W. It is driven by the PWM command, which allows complete rotation control between 0 and 2500 rpm, according to the datasheet provided by the manufacturer. An estimate to obtain the power of the electric fan at each rotation was used based on one of the fan law equations, which comes from applying the similarity theory to flow machines, Equation (3). To obtain the power of the electric fan at each rotation, an estimation based on one of the fan law equations comes from applying similarity theory to flow machines [36].

$$P_2 = P_1 \left(\frac{n_2}{n_1}\right)^3 \left(\frac{D_2}{D_1}\right)^5 \left(\frac{\rho_2}{\rho_1}\right) \quad (3)$$

As this is just a change in the rotation of the same electric fan, there is no variation in the fan diameter. The density of the working fluid was considered constant since the consumption tests were carried out in a temperature-controlled environment. A cubic curve of electrical power was obtained as a function of working rotation, Figure 7, and the results were calculated using Equation (3).

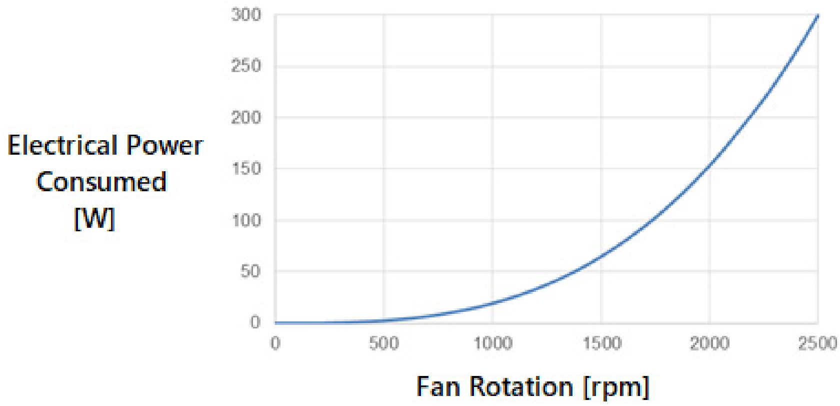

Figure 7. The electric fan consumes power.

Alternator mechanical efficiency: The mechanical efficiency of the alternator was considered constant at 60%. Current alternators have a typical average efficiency of around 70%, and their maps present values generally varying between 50% and 75%, depending on the operating point [37].

3.3. Intermediate Data

The intermediate data group contains all the information obtained through calculations in previous steps and is necessary for calculating the variables of interest. The following items report the types of information and the methods for obtaining them.

Airspeed at the radiator: The instantaneous average airflow speed through the radiator can be obtained directly from the location of the vehicle's operating points (Table 2) on the radiator airflow map.

System resistance curves: System resistance curves are the possible pump operating conditions for the cooling system to which it is applied. In this way, the mechanical power absorbed by the pump was obtained for any engine speed under open or closed thermostatic valve conditions, Figure 8. These are obtained by measuring and locating the points of the total flow curves in the water pump and on the power map (Figure 9), and the measurement error is 5%.

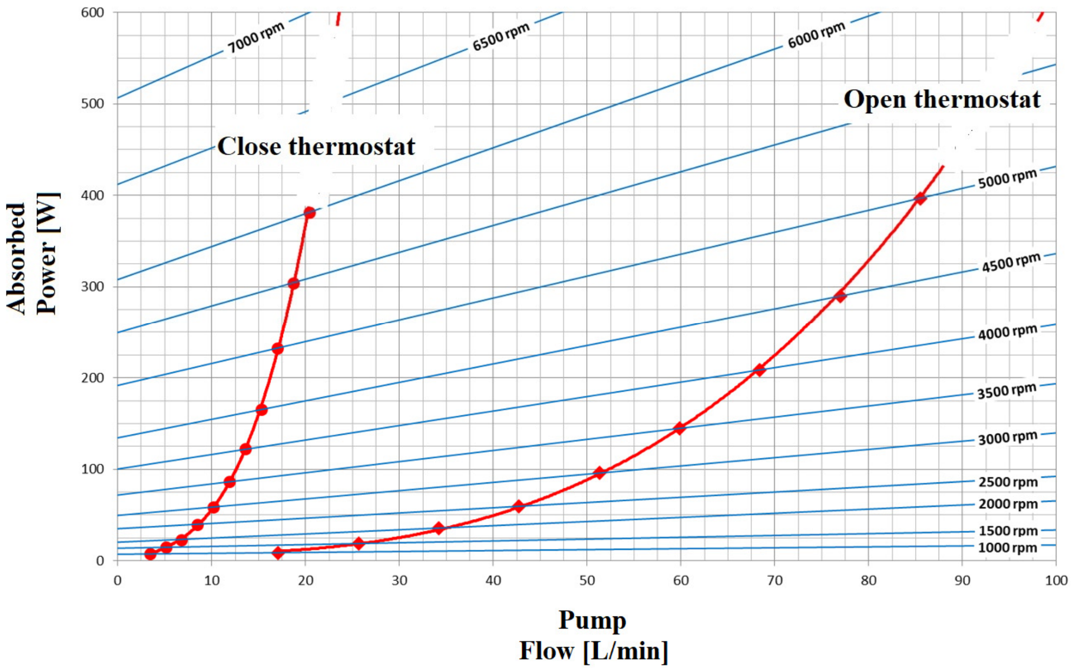

Figure 8. System resistance curves and power consumed per pump rotation.

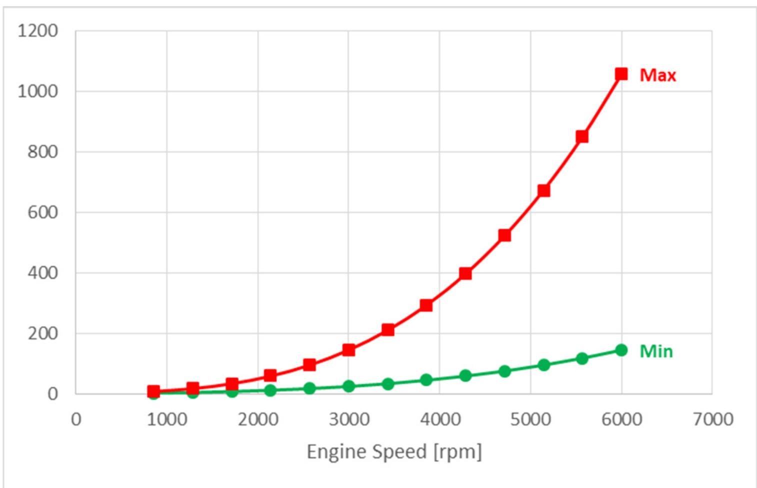

Figure 9. Power curves absorbed by the pump.

Electrical power demanded by the fan: Based on the power curve of the electric fan (Figure 6) and the vehicle's operating points (Table 2), the electrical power absorbed by the fan intended for vehicle cooling can be identified.

Water speed in the radiator: The water flow rate in the cooling system is obtained from the vehicle's operating points applied to the system's resistance curves (Figure 7). Here, the volumetric flow values through the radiator are converted into the average speed of water flow inside the heat exchanger through the cross-sectional area of the tubes, a constant value also obtained from the component's datasheet.

The mechanical power of the water pump: The system's resistance curves and the mechanical energy absorbed by the water pump during pumping work are obtained with the flow information. Figure 9 shows two curves of mechanical power the pump absorbs in pumping the coolant as a function of engine speed for the open thermostat for low and high flow conditions. The green curve represents the power pump operating in low flow mode (Min), and the red curve in high flow mode (Max). A significant reduction of 63% to 86% in the mechanical power absorbed is observed, depending on the engine speed.

Fan mechanical power: The shaft mechanical power absorbed by the fan is obtained by applying the efficiency (η_{alt}) of the alternator in converting mechanical power (P_{mec}) into electrical power (P_{ele}) demanded by the component according to Equation (4).

$$P_{mec} = \frac{P_{ele}}{\eta_{alt}} \tag{4}$$

3.4. Parameter Outputs

The output group contains the variables of interest. For this basic model, the claim is in thermal rejection in the radiator and the total mechanical power absorbed for cooling.

The thermal rejection in the radiator was calculated using air and water flow velocity data in the radiator and the radiator thermal rejection map; the instantaneous thermal rejection for the environment can be determined. As an equivalence criterion, it was assumed that the average thermal rejection must be kept constant between the baseline condition and the variable pump proposal, ensuring that the system performance is unaffected.

In the case of the mechanical power absorbed for cooling, the parasitic power of the cooling system is a measure of the total mechanical power obtained through the sum of the mechanical powers related to water pumping and air displacement by the fan. This parameter will allow calculating the amount of energy saved using the variable pump system and determining the best operating condition of the cooling system for each possible operating point.

3.5. Assessment of Operating Points

In possession of the thermal rejection and parasitic power results obtained from the basic model, the evaluation and mapping of the optimal operating conditions of the proposed cooling system were carried out, focusing on energy efficiency. This procedure was calculated considering the preliminary assessment and full assessment. In the case of the preliminary evaluation, a verification of points characteristic of the regular operation of a vehicle in urban driving was carried out. The points adopted were 15 km/h in 1st gear, 30 km/h in 2nd gear, and 50 km/h in 3rd gear. The reason for verifying these points was to understand whether an increase in air flow provided by activating the cooling system's electro-fan can compensate for the loss of thermal exchange in the radiator with a net reduction in parasitic power consumed. In the case of the full assessment, a complete survey of all possible operating points in each gear was carried out to identify the best water and airflow management strategies. Hence, it was possible to identify efficiency improvement trends, fan drive requirements, and ideal switching points between low and high water-pump flow. Based on the data obtained in the complete evaluation, a strategy for controlling the activation of the electric fan and water pump can be proposed depending on the vehicle's operating conditions.

3.6. Consumption Calculation Model

At this stage, the basic model was expanded to calculate thermal rejection and parasitic power for fixed operating points and determine the proposed vehicle's fuel consumption. Hence, the calculation is carried out based on the operating points of the vehicle with the proposed strategy while driving in the cycles presented on a theoretical basis. The configuration of the vehicle under study is used as a basis for the feasibility calculations of the proposal, which is a generic model from the Compact Hatches category. This segment comprised the following vehicles: Volkswagen Gol (São Paulo, Brazil), Nissan March (Rio de Janeiro, Brazil), Ford Ka (São Paulo, Brazil), Renault Sandero (Paraná, Brazil), Hyundai HB20 (São Paulo, Brazil), Fiat Argo (Minas Gerais, Brazil, and Chevrolet Onix Joy (São Paulo, Brazil). In this case, the base fuel consumption is determined by the consumption values in km/L presented in consultation with the PBEV (Brazilian Vehicle Labeling Program), which appears on the energy efficiency label issued by CONPET (National Program for the Rationalization of the Use of Petroleum Derivatives and Natural Gas), and values are adjusted by Equations (5) and (6) to reflect daily use, according to INMETRO Ordinance [38].

The flowchart in Figure 10 shows the complete calculation model, where the inclusion of new input and intermediate data can be seen, in addition to the output now being fuel consumption.

$$Cr_u = \frac{1}{0.00767212 + \frac{1.18053}{Ct_u}} \tag{5}$$

$$Cr_e = \frac{1}{0.0032389 + \frac{1.3466}{Ct_e}} \tag{6}$$

where Ct_u represents the Urban Test Consumption [km/L], Cr_e represents the Real Road Consumption [km/L], and Cr_u represents the Road Test Consumption [km/L].

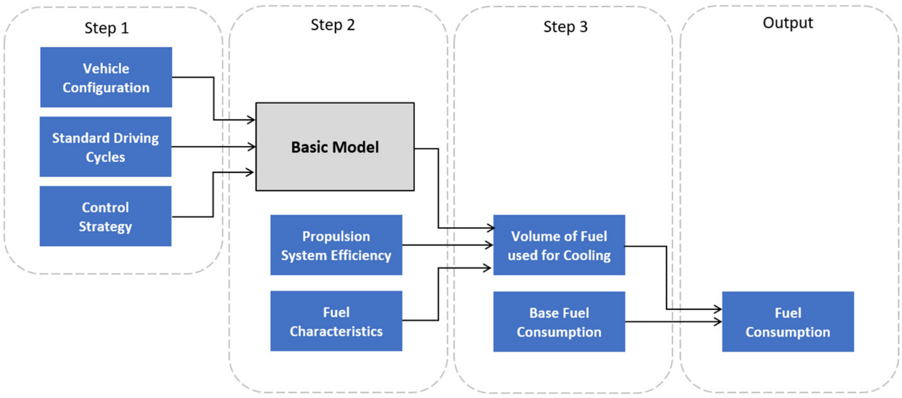

Figure 10. Flowchart of calculation methodology for the complete model.

For the proposed condition, fuel consumption was calculated by converting the chemical energy between the base and proposed vehicle by the difference in the amount of energy required in the original and proposed configuration into delta chemical energy of the fuel, resulting in a reduction in fuel consumption and mass of fuel burned, according to Equation (7).

$$CONS_2 = \frac{PCI \cdot dist}{\frac{PCI \cdot dist}{CONS_1} + (E_2 - E_1)} \tag{7}$$

4. Analysis and Discussion of Results

This section will show the results obtained from the optimized model developed through preliminary and complete evaluations, and finally, it will conduct the delta consumption simulation analysis.

4.1. Preliminary Assessment and Full Assessment

The preliminary assessment was conducted through the verification of the characteristic points of operation at 15 km/h (1st gear), 30 km/h (2nd gear), and 50 km/h (3rd gear), and also, the assessment of feasibility and potential for efficiency gains were carried out. Figure 11a,b presents the values of thermal rejection in the radiator and parasitic power of the cooling system as a function of the rotation of the electro-fan when operating with pump flow in low flow conditions (dotted lines) and compares them with the standard condition airflow with the electric fan turned off (solid lines).

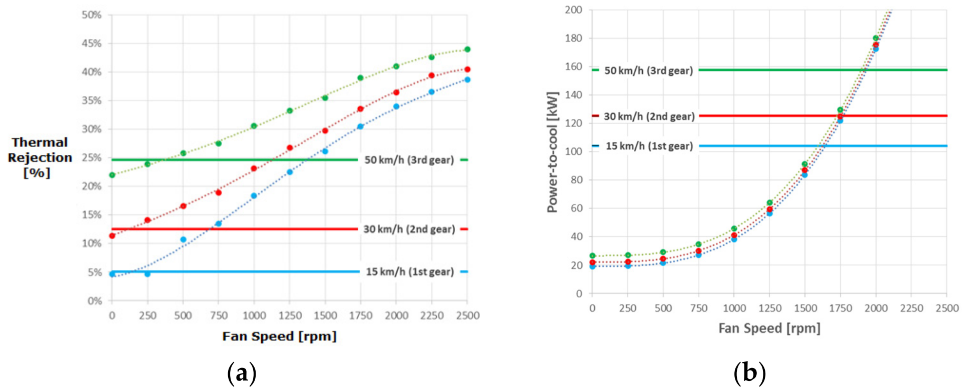

Figure 11. Energetic assessment: (**a**) Thermal rejection in the radiator; (**b**) Parasitic power of the cooling system.

It can be seen in Figure 11a that for conditions of 15 and 30 km/h, a fan drive of around 250 rpm is already capable of compensating for the loss of thermal rejection resulting from the reduced water flow. Similarly, the 50 km/h condition has higher rejection than the current condition, with a drive of around 500 rpm. This drive requires electrical power of less than 2.5 W to operate the fan. In the case of Figure 11b, a drastic reduction in the parasitic power consumed by the cooling system is noted, which remains at levels lower than those observed in current conditions until just above 1750 rpm, from which the reduction in flow in the pump is not justified. From an energy point of view, the electric fan's power consumption induces a higher level of energy consumption than the initial condition. At all three points of the analysis, a net reduction in mechanical power of more than 80% was possible, which indicates an attractive potential gain in urban driving cycles.

For the full assessment, a complete mapping of possible operating points was carried out at 1 km/h intervals for each gear, according to Table 3. For each operating point, thermal rejection and parasitic power were calculated at each electro-fan drive level varying between 250 and 2500 rpm in 250 rpm intervals and compared with the values obtained from the vehicle's base configuration. Figure 12 shows the behavior of the mechanical power required in 3rd gear in the water pump condition with a larger pulley ratio (high flow rate), represented by the thicker black line versus the smaller pulley ratio condition (low flow rate) with multiple drives of the electro-fan between 500 and 2500 rpm; thinner lines are written in green in regions where the power is lower than the base value and in red when higher.

Similarly, Figure 11b shows the behavior of thermal rejection in the radiator in 3rd gear. Again, the water pump condition with a higher pulley ratio (increased flow rate) can be indicated with the thicker black line and compared with the lower pulley ratio condition (low flow rate) in thinner lines, here written in green in the regions where thermal rejection is greater than the base value and in red when lower. The red areas of Figure 12a,b were situations where operating the pump at low flow was impossible and/or viable. Therefore, Figure 13a summarizes the conditions under which operation is in low flow mode and the power reduction obtained for each fan rotation, which may be interesting. Figure 13b shows the ideal rotation curves per gear.

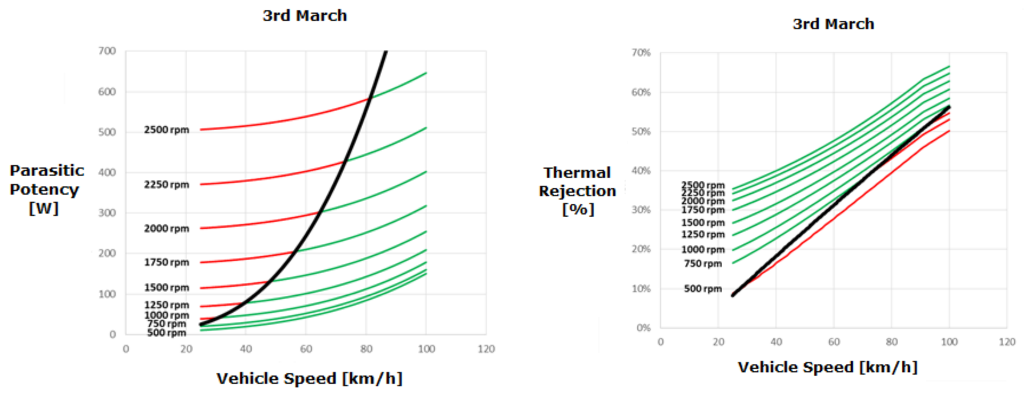

(**a**) (**b**)

Figure 12. Energetic assessment: (**a**) Parasitic power in 3rd gear. (**b**) Thermal rejection in 3rd gear.

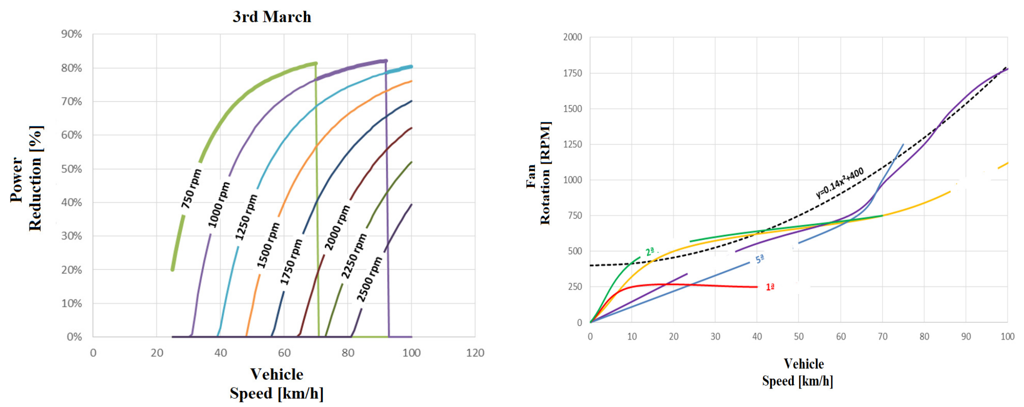

(**a**) (**b**)

Figure 13. Power evaluation: (**a**) Potential reduction in consumed power. (**b**) Electric fan drive strategy.

Observing that the smaller the electric fan drive, the lower the energy expenditure, it can be concluded that in 3rd gear, operating from 25 km/h to 100 km/h, it is possible to reduce the level of parasitic power consumed in cooling by lowering the water pump flow with complementary electro-fan drive at 750 rpm between 25 and 70 km/h, 1000 rpm between 70 and 92 km/h, and 1250 rpm between 92 and 100 km/h. This gear's parasitic power reduction varies between 20% and 82%. From this information, a second-degree polynomial function was generated that determines the ideal rotation speed of the electric fan depending on the vehicle speed, setting the minimum rotation at 400 rpm (16% activation). The proposed function, therefore, determines the activation of the electric fan continuously depending on the speed, with rotations between 400 and 1296 rpm in the range of 0 to 80 km/h, with the maximum driving power of the electric fan (FAN) of up to 41.8 W, equivalent to 52% drive (Duty Cycle). Table 4 presents the values used to create the fan rotation map as a function of vehicle speed.

Table 4. Fan drive map depending on speed.

Fan Map as a Function of Vehicle Speed (Low Flow Pump)												
Speed	[km/h]	0	10	20	30	40	50	60	70	80	90	100
Duty Cycle FAN	[%]	16	17	18	21	25	30	36	43	52	61.36	72
Rotation FAN	[rpm]	400	414	456	526	624	750	904	1086	1296	1534	1800
Power FAN	[w]	1.2	1.4	1.8	2.8	4.7	8.1	14.2	24.6	41.8	69.3	112.0

This electro-fan activation should only be applied when the engine has the thermostatic valve completely open or close to it, as it will be using the system's water flow at its maximum capacity, reaching high levels of heat exchange saturation on the radiator's air side. Another critical point is that there is no need to cool the engine at lower temperatures, and there is no point in increasing energy expenditure with the fan in these situations. Therefore, in situations where the temperature of the cooling fluid is slightly lower than the temperature at which the thermostatic valve opens, there may be a criticality in operating the pump in its low-speed position since the lower flow rate may cause regions of more significant stagnation of the cooling fluid, and, with the engine under high load, localized points of high temperature or hot spots can be observed. These points can have several harmful effects, from inducing pre-ignition in the combustion chamber to the nucleation of bubbles and vapor films in these hot spots, with severe risks of irreversible damage or even engine breakdown. A switching strategy was established between low- and high-flow positions depending on the load requested by the driver. This work adopted a limit value of 70% load for operation with reduced flow.

Table 5 presents a base fan activation condition considering its activation from 96 °C, which would begin the nominal temperature range where the electric fan controls the temperature since the thermostat is already open to the maximum.

Table 5. Base calibration of electro fan.

Fan Basemap												
Water Temperature	[°C]	95	95	97	98	99	100	101	102	103	104	105
Duty Cycle FAN	[%]	0	20	30	40	50	60	170	80	190	100	100
Rotation FAN	[rpm]	0	500	750	1000	1250	1500	1750	2000	2250	2500	2500
Power FAN	[W]	0	2.4	8.1	19.2	37.5	64.8	102.9	153.6	1218.7	300.0	300.0

In the temperature condition where the current car would already request electro-activation, the vehicle does not have a loss of thermal rejection; hence, an analysis was made of what the fan rotation increment should be to conserve the thermal rejection potential. Finally, the characteristic points in Table 6 were simulated in the current configuration, and the minimum electric fan requirement was identified to maintain the same or greater capacity with reduced water flow.

Table 6. Characteristic points.

March	**Speed**
1st	15 km/h
2nd	30 km/h
3rd	50 km/h
4th	65 km/h
5th	80 km/h

It was found that, on average, the fan rotation must be increased by 750 rpm to guarantee the same radiator performance. The maximum temperature that allows operation with reduced flow in the pump must be 98 °C. Above this, it is not possible to maintain the performance cooling system, and it is recommended to operate the pump continuously at maximum flow. Table 7 shows the electric fan activation values by temperature.

According to Tables 6 and 7, once the temperature exceeds 95 °C, the electro-activation required by temperature will always be greater than the activation requested by speed. Therefore, Figure 14 shows the optimized scheme of the pump and fan controls.

Table 7. Temperature calibration for low pump flow.

Fan Map as a Function of Water Temperature (Low Flow Pump)												
Water Temperature	[°C]	95	96	97	98	99	100	101	102	103	104	105
Duty Cycle FAN	[%]	0	50	60	70	100	100	100	100	100	100	100
Rotation FAN	[rpm]	0	1250	1500	1750	250	250	250	250	250	250	250
Power FAN	[W]	0	37.5	64.8	102.9	300	300	300	300	300	300	300

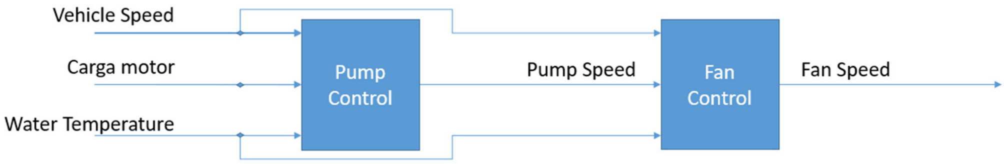

Figure 14. Optimized control scheme temperature calibration for low pump flow.

Tables 8 and 9 detail the proposed control logic for the pump and fan, respectively, represented by the blue blocks in Figure 13.

Table 8. Water pump drive diagram.

<table>
<tr><th colspan="2" rowspan="2">Pump Control Logic</th><th>Cold</th><th>Warm</th><th>Nominal (Thermostatic Control)</th><th>Nominal (Fan Control)</th><th>Heated</th></tr>
<tr><th>$T \leq 70\ ^\circ C$</th><th>$70\ ^\circ C < T \leq 85\ ^\circ C$</th><th>$85\ ^\circ C < T \leq 95\ ^\circ C$</th><th>$95\ ^\circ C < T \leq 98\ ^\circ C$</th><th>$T > 98\ ^\circ C$</th></tr>
<tr><td rowspan="3">Low Flow Pump</td><td>Engine load ≤ 70%</td><td rowspan="4">Low Flow</td><td colspan="3">Low Flow</td><td rowspan="4">High Flow</td></tr>
<tr><td>Engine load > 70%</td><td>High Flow</td><td colspan="2" rowspan="3">High Flow</td></tr>
<tr><td>Engine load ≤ 70%</td><td>Low Flow</td></tr>
<tr><td>High Flow Pump</td><td>Engine load > 70%</td><td>High Flow</td></tr>
</table>

Table 9. Radiator fan drive diagram.

<table>
<tr><th colspan="2" rowspan="2">Fan Control Logic</th><th>Cold</th><th>Warm</th><th>Nominal (Thermostatic Control)</th><th>Nominal (Fan Control)</th><th>Heated</th></tr>
<tr><th>$T \leq 70\ ^\circ C$</th><th>$70\ ^\circ C < T \leq 85\ ^\circ C$</th><th>$85\ ^\circ C < T \leq 95\ ^\circ C$</th><th>$95\ ^\circ C < T \leq 98\ ^\circ C$</th><th>$T > 98\ ^\circ C$</th></tr>
<tr><td rowspan="3">Low Flow Pump</td><td>OFF</td><td>X</td><td>X</td><td></td><td></td><td></td></tr>
<tr><td>Speed Map</td><td></td><td></td><td>X</td><td></td><td></td></tr>
<tr><td>Temperature Map</td><td></td><td></td><td></td><td>X</td><td></td></tr>
<tr><td>High Flow Pump</td><td>Temperature Map</td><td></td><td></td><td></td><td>X</td><td>X</td></tr>
</table>

4.2. Consumption Delta Simulation

Finally, control strategies were implemented considering the base consumption information and operating points obtained. As shown in Table 10, a 1.0% improvement in consumption can be seen on average for the cycles evaluated, with 1.2% to 1.5% in strictly urban cycles and in the order of 0.3% to 0.5% in road or aggressive driving cycles, such as the HWFET and the RTS95.

4.3. Final Remarks from the Proposal Implementation

This study's contributions to the current state of research in the field, specifically regarding energy efficiency in small vehicles (focusing on consumption and power), can be validated. The initial findings affirm a noteworthy enhancement through applying this methodology in a verified case, encompassing various urban and low-speed cycles. An estimated reduction in consumption from 1.2% to 1.4% was observed primarily due to decreased parasitic power attributed to the fuel pump. Comparable results were identified in the literature, notably in the NEDC cycle by Yuan et al. [19], who simulated and tested a 1.5 T vehicle engine, achieving a similar reduction in consumption through optimization of the cooling system under varying operating conditions. This confirms the suitability and practicality of the proposed implementation methodology.

Table 10. Delta Consumption.

Cycle	Consumption Delta [%]
FTP75	1.23
HWFET	0.27
NEDC	1.18
WLTP	0.78
LA	0.91
NY	1.43
ARTEMIS	1.49
RTS95	0.52

Furthermore, a comparative analysis of the results was conducted, focusing on two performance metrics: the reduction in parasitic power and the improvement in consumption. Numerous works in the literature have explored strategies aimed at maximizing these metrics to enhance overall engine performance, such as Turabimana et al. [18], where an integration of an active engine cooling system with an alloy-based thermostat to achieve energy gains was conducted, Yuan [19]'s optimization of the heat dissipation system for efficient vehicle and engine cooling, and Naderi et al. [16]'s enhancement of efficiency through intelligent pump control. Table 11 presents a comparison of the literature.

Table 11. Comparative analysis.

Work	Results		
	Power Reduction	Consumption Improvement	Consumption Cycle
This proposal	40%	0.73%	WLTC
	53%	1.18%	NEDC
[14]	12–22%	0.4%	WLTC
[16]	30.0%	0.6%	WLTC
[18]	44.3%	2.1%	Uninformed
[19]	50.0%	1.1%	NEDC

The proposed methodology demonstrated an average power reduction comparable to literature-sampled works for the WLTC and NEDC cycles. A distinctive result was observed in Cipollone et al. [14]'s study, where a vane pump replaced the conventional centrifugal pump to reduce parasitic power in the WLTC cycle.

Regarding consumption improvement, the proposed methodology yielded values consistent with those in Cipollone et al. [14], Naderi et al. [16], and Yuan et al. [19], approximately 1.2%, though slightly lower than Turabimana et al. [18]'s study. Notably, the cycle details in Turabimana et al. [18]'s study were not disclosed, possibly contributing to the variance. Despite this, the obtained results align coherently and signify significant gains for this specific application, holding substantial importance for the transport sector.

5. Conclusions

The proposed system presents theoretical technical feasibility for practical application as a fuel consumption technology. Among the most relevant results are:

- The smaller the fan drive, the lower the energy expenditure, reducing the parasitic power consumed in cooling as much as possible, reducing the pump flow of water with a complementary drive of the electro-fan. The parasitic power reduction varies and ranges between 20% and 82% in 3rd gear;
- From the view of practical implementation, the electric fan activation must only be applied when the engine has the thermostatic valve completely open or close to it, as the system's water flow will be used at its maximum capacity, reaching high levels of saturation of heat exchange on the air side of the radiator;
- Considering long-term implications, in the case where the coolant temperature was slightly lower than the opening temperature of the thermostatic valve, criticalities may arise when operating the pump in its low-speed position. The lower flow rate can result in regions of significant fluid stagnation, leading to localized high-temperature points or hot spots under high engine load;
- A switching strategy between low- and high-flow positions was established based on the load requested by the driver to ensure sustained long-term performance. This research implemented a limit value of 70% load for operation with reduced flow, thereby mitigating potential challenges associated with pump operation in its low-speed position;
- Regarding practical viability, the results demonstrate the potential of the proposal presented and its technical feasibility for practical application as a fuel consumption technology for small vehicles;
- The fan rotation must be increased by 750 rpm to guarantee the same radiator performance, and the maximum temperature that allows it to operate with the reduced flow in the pump must be 98 °C; above this, it was not possible to maintain the cooling performance, and it is recommended to operate with the pump at maximum flow continuously;
- Regarding the cost-benefit analysis and safety, these conclusions represent significant advances in energy efficiency and fuel consumption in combustion vehicles, contributing to developing more sustainable and economically viable technologies.

In addition to the joyous final considerations found, a couple of studies could be conducted to continue the understanding and optimization of this issue:

✓ To couple a thermal model of the vehicle's cooling system to the parasitic power calculation to evaluate the impacts of reduced water circulation during the initial engine warm-up, with a likely improvement in the heating rate and consequent reduced internal friction during cold starts.

✓ Optimizing the pump drive depends on the air conditioning operation, which sometimes requires the electric fan to operate at levels much higher than needed to cool the engine, consequently lowering the engine temperature by up to 10 °C.

Author Contributions: Conceptualization, P.H.A.B., J.Â.P.d.C. and A.A.V.O.; methodology, P.H.A.B., J.Â.P.d.C. and A.A.V.O.; software, P.H.A.B., J.Â.P.d.C. and A.A.V.O.; validation, P.H.A.B., J.Â.P.d.C. and A.A.V.O.; formal analysis, P.H.A.B.; investigation, P.H.A.B.; resources, P.H.A.B., J.Â.P.d.C., A.A.V.O. and G.N.P.L.; data curation, P.H.A.B.; writing—original draft preparation, P.H.A.B., J.J.U., P.S.A.M. and A.A.V.O.; writing—review and editing, J.Â.P.d.C., G.N.P.L. and A.A.V.O.; visualization, supervision, J.Â.P.d.C., G.N.P.L., A.A.V.O. and P.S.A.M.; project administration, J.Â.P.d.C., G.N.P.L., A.A.V.O., J.J.U. and P.S.A.M.; funding acquisition, J.Â.P.d.C., G.N.P.L. and A.A.V.O. All authors have read and agreed to the published version of the manuscript.

Funding: The second and third authors are funded by the IFPE and CNPq through (N# 3303417/2022-6), respectively.

Data Availability Statement: Data are contained within the article.

Acknowledgments: The authors thank the PPGEM/UFPE and Capes for supporting the master's dissertation. The second and third authors thank the IFPE and CNPq for their support (N# 3303417/2022-6), respectively.

Conflicts of Interest: The authors declare no conflict of interest.

Nomenclature

C	Fuel consumption	[L/100 km]
m_{HC}	Mass of HC emitted	[g/km]
m_{ETOH}	Mass of ethanol emitted	[g/km]
m_{CO}	Mass of CO emitted	[g/km]
m_{CO_2}	Mass of CO_2 emitted	[g/km]
$\%V_{gs}$	Percentage, by volume at 20 °C, of gasoline in the fuel used	[-]
$\%V_{ETOH}$	Percentage, by volume at 20 °C, of ethanol in the fuel used	[-]
$\%V_{H_2O}$	Percentage, by volume at 20 °C, of water in the fuel used	[-]
A	Autonomy per Liter	[km/L]
P	Power	[W]
n	Rotation	[rpm]
D	Diameter	[mm]
Cr_u	Real urban consumption	[km/L]
Ct_u	Urban test consumption	[km/L]
Cr_e	Real road consumption	[km/L]
Ct_e	Road test consumption	[km/L]
$CONS_1$	Original energy consumption	[km/L]
$CONS_1$	Proposed Energy consumption	[km/L]
PCI	Fuel Lower Calorific value	[MJ/L]
$dist$	Distance traveled during the test	[km]
E_1	Original chemical energy	[MJ]
E_2	Proposed Chemical energy	[MJ]

Greek Letters

ρ	Fluid density	[kg m^3]
η_{alt}	Alternator efficiency	[-]

Subscripts

CFD	Computational Fluid Dynamics
ANP	National Agency for Petroleum, Natural Gas and Biofuels
RPM	Revolutions per minute
ICCT	*International Council on Clean Transportation*
3D	Three-dimentional
1D	One-dimentional
HC	Hidrocarboneto
VDE	Vehicle Demand Energy
AGS	Active Grille Shutters
EPA	*United States Environmental Protection Agency*
FTP	*Federal Test Procedure*
MDIC	Ministry of Development, Industry and Foreign Trade
MESAU	*Minimum Engine Speed After Upshift*
NEDC	*New European Driving Cycle*
PBEV	Brazilian Vehicle Labeling Program
PME	Average Effective Pressure
PSE	*Propulsion System Efficiency*
PWM	*Pulse Width Modulation*
RDE	*Real Driving Emissions*
UE	European Union
VSE	*Vehicle Spent Energy*
VVT	*Variable Valve Timing*
WLTC	*Worldwide Harmonised Light Vehicles Test Cycle*

References

1. Fatiguso, M.; Valenti, A.R.; Ravelli, S. Comparative energy performance analysis of micro gas turbine and internal combustion engine in a cogeneration plant based on biomass gasification. *J. Clean. Prod.* **2023**, *434*, 2024. [CrossRef]
2. Syed, Z.A.; Wagner, J.R. Modeling and Control of a Multiple-Heat-Exchanger Thermal Management System for Conventional and Hybrid Electric Vehicles. *Designs* **2023**, *7*, 19. [CrossRef]
3. Śliwiński, K.; Szramowiat, M. Development of cooling systems for internal combustion engines in the light of the requirements of modern drive systems. *IOP Conf. Ser. Mater. Sci. Eng.* **2018**, *421*, 042078. [CrossRef]
4. Xu, J.; Cheng, K.; Dang, C.; Wang, Y.; Liu, Z.; Qin, J.; Liu, X. Performance comparison of liquid metal cooling system and regenerative cooling system in supersonic combustion ramjet engines. *Energy* **2023**, *275*, 127488. [CrossRef]
5. Balali, Y.; Stegen, S. Review of energy storage systems for vehicles based on technology, environmental impacts, and costs. *Renew. Sustain. Energy Rev.* **2021**, *135*, 110185. [CrossRef]
6. Leach, F.; Kalghatgi, G.; Stone, R.; Miles, P. The scope for improving the efficiency and environmental impact of internal combustion engines. *Transp. Eng.* **2020**, *1*, 100005. [CrossRef]
7. Kim, C.H.; Jun, S.-B.; Yoon, H.-J.; Kim, N.-H.; Jung, H.-C.; Kim, R.-E.; Jung, S.-Y. Calculation of Parasitic Capacitance to Analyze Shaft Voltage of Electric Motor with Direct-Oil-Cooling System. *Processes* **2022**, *10*, 1541. [CrossRef]
8. Li, W.; Wang, N.; Garg, A.; Gao, L. Multi-objective optimization of an air cooling battery thermal management system considering battery degradation and parasitic power loss. *J. Energy Storage* **2023**, *58*, 106382. [CrossRef]
9. Tian, H.; Zhang, H.; Yin, Z.; Liu, Y.; Zhang, X.; Xu, Y.; Chen, H. Advancements in compressed air engine technology and power system integration: A comprehensive review. *Energy Rev.* **2023**, *2*, 100050. [CrossRef]
10. Wu, Z.; Wu, J.; Kang, Z.; Deng, J.; Hu, Z.; Li, L. A review of water-steam-assist technology in modern internal combustion engines. *Energy Rep.* **2021**, *7*, 5100–5118. [CrossRef]
11. Chen, Y.; Lawell, C.Y.C.L.; Wang, Y. The Chinese automobile industry and government policy. *Res. Transp. Econ.* **2020**, *84*, 100849. [CrossRef]
12. Yoo, S.; Wakamori, N.; Yoshida, Y. Preference or technology? Evidence from the automobile industry. *Transp. Res. Part D Transp. Environ.* **2021**, *96*, 102846. [CrossRef]

13. Niquito, T.W.; Carraro, A. Efeitos do programa inovar-auto sobre a indústria de veículos no Brasil. *Econ. Apl.* **2021**, *25*, 249–292. [CrossRef]
14. Cipollone, R.; Bianchi, G.; Di Battista, D.; Fatigati, F. Fuel economy benefits of a new engine cooling pump based on sliding vane technology with variable eccentricity. *Energy Procedia* **2015**, *82*, 265–272. [CrossRef]
15. Fatigati, F.; Di Battista, D.; Cipollone, R. Design improvement of volumetric pump for engine cooling in the transportation sector. *Energy* **2021**, *231*, 120936. [CrossRef]
16. Naderi, A.; Qasemian, A.; Shojaeefard, M.H.; Samiezadeh, S.; Younesi, M.; Sohani, A.; Hoseinzadeh, S. A smart load-speed sensitive cooling map to have a high- performance thermal management system in an internal combustion engine. *Energy* **2021**, *229*, 120667. [CrossRef]
17. Haghighat, A.K.; Roumi, S.; Madani, N.; Bahmanpour, D.; Olsen, M.G. An intelligent cooling system and control model for improved engine thermal management. *Appl. Therm. Eng.* **2018**, *128*, 253–263. [CrossRef]
18. Turabimana, P.; Sohn, J.W.; Choi, S.B. A Novel Active Cooling System for Internal Combustion Engine Using Shape Memory Alloy Based Thermostat. *Sensors* **2023**, *23*, 3972. [CrossRef]
19. Yuan, Z.; An, T.; Pan, Y.; Chen, H.; Liu, Y.; Zhan, C. Simulation Research on Parameters Matching of Vehicle Engine Cooling System Based on AMEsim. *J. Phys. Conf. Ser.* **2022**, *2395*, 012014. [CrossRef]
20. Addo, K.D.; Davis, F.; Fiagbe, Y.A.K.; Andrews, A. Machine learning for predictive modelling of the performance of automobile engine operating without coolant thermostat. *Sci. Afr.* **2023**, *21*, e01802. [CrossRef]
21. Faraj, J.; Chahine, K.; Mortada, M.; Lemenand, T.; Ramadan, H.S.; Khaled, M. Eco-Efficient Vehicle Cooling Modules with Integrated Diffusers—Thermal, Energy, and Environmental Analyses. *Energies* **2022**, *15*, 7917. [CrossRef]
22. Gupta, M.K.; Niesłony, P.; Sarikaya, M.; Korkmaz, M.E.; Kuntoğlu, M.; Królczyk, G.M.; Jamil, M. Tool wear patterns and their promoting mechanisms in hybrid cooling assisted machining of titanium Ti-3Al-2.5V/grade 9 alloy. *Tribol. Int.* **2022**, *174*, 13. [CrossRef]
23. Kalinichenko, A.; Havrysh, V.; Hruban, V. Heat recovery systems for agricultural vehicles: Utilization ways and their efficiency. *Agriculture* **2018**, *8*, 199. [CrossRef]
24. Alktranee, M.; Bencs, P. Factors affecting nanofluids behaviour: A review. *Int. Rev. Appl. Sci. Eng.* **2023**, *14*, 241–255. [CrossRef]
25. Bencs, P.; Alktranee, M. The potential of vehicle cooling systems. *J. Phys. Conf. Ser.* **2021**, *1935*, 012012. [CrossRef]
26. Brayner, P.H.A. *Melhoria de Consumo de Combustível de um Veículo a Combustão Através de Redução na Potência Parasítica do Sistema de Arrefecimento [Improving the Fuel Consumption of a Combustion Vehicle Through Reduction in the Parasitic Power of the Cooling System]*; Federal University of Pernambuco–UFPE: Recife, Brazil, 2022.
27. ABNT. *NBR 10312–Veículos Rodoviários Automotores Leves–Determinação da Resistência ao Deslocamento por Desaceleração Livre em Pista de Rolamento e Simulação em Dinamômetro [Light Motor Road Vehicles–Determination of Resistance to Displacement by Free Dece]*; ANBT: São Paulo, Brazil, 2019.
28. ABNT. *NBR 6601–Veículos Rodoviários Automotores Leves–Determinação de Hidrocarbonetos, Monóxido de Carbono, Óxidos de Nitrogênio e Dióxido de Carbono no gás de Escapamento [Light Motor Vehicles–Determination of Hydrocarbons, Carbon Monoxide, Nitrogen Oxide]*; ANBT: São Paulo, Brazil, 2001.
29. ABNT. *NBR 7024–Veículos Rodoviários Automotores Leves–Medição do Consumo de Combustível [Light Motor Vehicles–Measuring Fuel Consumption]*; ANBT: São Paulo, Brazil, 2002; p. 13.
30. United States Environmental Protection Agency. *Dynamometer Drive Schedules*; EPA: Washington, DC, USA, 2021. Available online: https://www.epa.gov/vehicle-and-fuel-emissions-testing/dynamometer-drive-schedules (accessed on 12 March 2021).
31. Cornell University. EPA Dynamometer Driving Schedules. 2021. Available online: https://www.law.cornell.edu/cfr/text/40/86.115-78 (accessed on 15 October 2021).
32. Institute for Environment and Sustainability. *Regulated Emissions of a Euro 5 Passenger Car Measured over Different Driving Cycles*; Institute for Environment and Sustainability: Ispra, Italy, 2010.
33. DieselNet. Emission Test Cycles: Worldwide Engine and Vehicle Test Cycles. 2021. Available online: https://dieselnet.com/standards/cycles/index.php#us-ld (accessed on 12 March 2021).
34. X-ENGINEER.ORG. EV Design–Energy Consumption. 2021. Available online: https://x-engineer.org/ev-design-energy-consumption/ (accessed on 12 March 2021).
35. ABNT. *NBR 8689–Veículo Rodoviários Automotores Leves–Combustíveis Para Ensaio [Light Motor Vehicles–Test Fuels]*; ABNT: São Paulo, Brazil, 2012; pp. 1–8.
36. Henn, É.A.L. *Máquinas de Fluido [Fluid Machines]*, 4th ed.; Universidade Federal de Santa Maria: Santa Maria, Brazil, 2019.
37. Doffe, L.; Kadiri, M. Alternator contribution to CO_2 emission reduction policies. In Proceedings of the XIX International Conference on Electrical Machines—ICEM, Rome, Italy, 6–8 September 2010. [CrossRef]
38. INMETRO. *Metodologia Para Divulgação de Dados de Consumo Veicular [Methodology for Disclosing Vehicle Consumption Data]*; INMETRO: Brasilia, Brazil, 2009; p. 2009.